Deep LSTM Neural Networks in Kinematic Estimation of the Finger Interphalangeal Joint's Angles Using Surface Electromyogram Signals

Masoud Saheb Jameyan, Mohammad Ali Ahmadi Pajouh*, and Mohammad Hassan Moradi

Department of Biomedical Engineering, Amirkabir University of Technology, Tehran, Iran

*Correspondence e-mail: pajouh@aut.ac.ir.

Abstract

In rehabilitation, hand robotics, and kinesiology, a crucial challenge is establishing a connection between surface electromyogram (sEMG) signals and the kinematics of joints and upper limbs. The present research introduces a deep recurrent neural network regressor that uses LSTM (Long Short Term Memory) and GRU (Gated Recurrent Unit) cells, leveraging sEMG signals to estimate finger joint angles. This investigation used the DB2 series of the Ninapro dataset. Remarkably, many joint angles can be estimated with up to 97% accuracy when based on the correlation coefficient criterion. This indicates a strong positive correlation between the estimated values and the actual values of these joints. However, it is significant to note that there is a trade-off between accuracy, learning time, and the number of parameters used, which varies based on the type of cells employed in the network. Using deep LSTM neural networks, it is possible to estimate the interphalangeal joint angles of the fingers with an accuracy of 97%. LSTM cells offer more precise predictions but require more learning time and parameters than GRU cells. The study also explores the significance of efficient muscles in executing movements, potentially influencing the varying estimation accuracy among different joints.

Keywords: Deep learning; finger joint angle; LSTM; GRU; estimation.

1. Introduction

The human hand plays a critical role in daily activities, as it is responsible for most of the tasks we perform. Volitional and tactile actions heavily rely on our hands. Smooth and uninterrupted hand movements are essential for various activities, but there can be instances where these movements are hindered for various reasons. To address such issues, it becomes necessary to continuously estimate the movements of the upper limbs and the angles of the joints. There are several practical applications for this continuous estimation, including hand rehabilitation following stroke or sports injuries, as well as for diagnosis, treatment, and monitoring of neurological diseases [1]. Additionally, this estimation process contributes to the development of rehabilitation robots and prostheses, aiming to create seamless and coordinated movements [2]. The surface electromyography (sEMG) signal refers to the electric potentials generated by the depolarization of muscle fiber membranes, which can be detected by electrodes placed on the skin surface. This signal carries valuable information that finds numerous applications in neuromuscular physiology and movement control [3]. One such application involves identifying the intention of movement, where the sEMG signal is used to establish a connection between muscle contractions and kinematics.

There are various methods available for continuous estimation and regression of hand movements. One such method is musculoskeletal models (MSM), which employs a skeletal model and incorporates the mechanical model of muscles. Using muscle synergies extracted from EMG data, He et al. constructed a musculoskeletal model to predict the joint angles of the thumb, index finger, middle finger, and wrist [4]. Kim et al. devised a muscle synergy and musculoskeletal model to estimate wrist joint angles. They used a seven-channel EMG signal to estimate wrist joint movements in two dimensions. An analysis of the EMG signals was conducted utilizing the musculoskeletal model and the synergy-based linear regression model [5]. However, this approach has limitations as it requires determining numerous parameters during testing, making it less suitable for continuous estimation of joint angles and movements [6].

In addition to MSM, traditional machine learning methods have been employed for estimating sEMG-based finger joint angles. Gao et al. employed the least square support vector machine (LSSVM) with time-delayed features of sEMG to estimate continuous wrist palmar flexion-extension angles. In order to increase the precision and speed of the least square support vector machine, they presented two feature engineering strategies [7]. Savithri et al. used partial least squares discriminant analysis to identify hand actions from single-channel sEMG signals [8]. Stapornchaisit et al. performed finger angle estimation using independent component analysis (ICA) coupled with a linear regression model (LRM). They employed high-density electrodes [9]. Veer et al. identified and classified upper limb motions using PCA [10]. Zhang et al. introduced an estimation approach utilizing Sparse Pseudo-input Gaussian Process (SPGP) regression to predict kinematics from sEMG signals. The joint angles of the metacarpophalangeal (MCP) were estimated. Six grasping motions were explored [11]. Chen et al. investigated finger kinematics based on motor unit discharge times. They used high-density electrodes to record the EMG signals from the forearm muscles. Using a blind-source separation technique, EMG signals were separated down into motor units. [12]. Hu et al. explored muscle synergy during dynamic finger movements. They estimated the movement of four fingers using seventy-two electrodes [13]. Pallotti et al. performed a comparison between the measurement of finger joint angles using a myoelectric armband and data gloves. They employed the Matlab regression learner for four movements [14]. Dai et al. predicted joint angles with a polynomial regressor. They recorded the sEMG data using a grid of 160 high-density electrodes. The resultant neural drive signals were used in a second-order polynomial regression to estimate the MCP joint angle [15]. Roy suggested an MCP joint finger kinematic prediction model based on motor units. To record the EMG signals, an 8 × 16 electrode array was placed over the flexor muscle [16]. The majority of these endeavors necessitate the fine-tuning of numerous parameters and substantial domain expertise [17].

An alternative, neural network structures have also been employed for this purpose by researchers. Batayneh et al. established a nonlinear mapping between sEMG signals and hand angles using neural networks [18]. Gao et al. used a controller based on the nonlinear autoregressive with exogenous inputs (NARX) model to estimate finger joint angles from sEMG signals [19]. However, these methods require access to high-quality data and involve the setup of numerous parameters [20].

The field of medical engineering has experienced significant advancements as a result of deep learning techniques [21-22]. The utilization of deep learning for hand gesture recognition has resulted in notable progress. Wen et al. proposed a convolutional neural network (CNN) framework for estimating neural drives in isometric contraction tasks [23]. Guo et al. employed a convolutional structure to predict finger kinematics [24]. Ma et al. employed LSTM (Long Short Term Memory) to predict knee joint angles based on sEMG signals [6]. Wang et al. used LSTM networks to predict upper limb joint angles. They examined six grasping movements [25]. Chen et al. investigated the upper shoulder elbow joints in three dimensions using an LSTM

network [26]. Avian et al. developed a regressor based on LSTM and manifold learning to estimate finger movements. The MCP joint angles study was performed by them [27].

In recent years, LSTM networks have drawn more attention from data scientists due to their ability to resolve the vanishing gradient issue that traditional recurrent networks typically encounter. LSTM networks use gate functions to govern state dynamics, which allows them to collect and simulate temporal data dependencies. Deep LSTM neural networks are the most effective method for estimating finger joint angles because the nature of sEMG signals is stochastic and time-dependent. The use of the network based on LSTM cells and one of its most useful variations, GRU, has been examined in this study. For the majority of the joints, the obtained results show that the kinematic assessment of the joints is 97% accurate. In comparison to all the previously described approaches, high accuracy was attained for all MCP, proximal interphalangeal (PIP), and distal interphalangeal (DIP) joints of the thumb, index, middle, ring, and little fingers in the current study, which was carried out using just ten electrodes. Based on the findings, the forearm muscles that are beneficial to moving finger joints have been identified, and the physiological basis for this has been studied. Selecting the appropriate window length for the windowing approach is one of the crucial problems in LSTM networks. The ideal window length has also been looked into in this research. The rest of the paper introduces the methods used, such as the dataset, LSTM and GRU (Gated Recurrent Unit) structures, network architecture, and evaluation criteria. The results are discussed in the third section, followed by a discussion in the fourth section.

2. Methodes

2.1. Data Base

In this study, the Ninapro DB2-exercise B database has been used, which consists of kinematic and sEMG data from the upper limbs of 40 healthy individuals [28]. This class includes wrist, grasping, basic movements, and hand postures. From the previously indicated set, six hand configurations related to isometric and isotonic movements were chosen for this study and joint angles were estimated during these movements. The Ninapro DB2 database is freely accessible to the public [29]. Muscle activity was recorded using 12 electrodes: eight around the forearm, two on the flexor and extensor digitorum muscles, and two on the biceps and triceps. EMG signals were sampled at 2 kHz. Figure 1(A) illustrates the placement of the electrodes. In this study, only data from the first ten electrodes (red and blue) were used to estimate finger angles during flexion and extension. The two green electrodes placed on the triceps and biceps muscles were excluded, as these muscles do not contribute to finger movement. Figure 1(B) displays the chosen movements.
Kinematic data was collected using a CyberGlove II dataglove with 22 sensors that capture finger and thumb joint movements, including flexion and abduction, as shown in Figure 1(C) [30]. The study focuses on analyzing joint angles between finger phalanges.

Figure 1: (A): The placement of electrodes [28]. (B): Selected movements of the fingers [29]. (C): The placement of bending sensors [30]

2.2. LSTM and GRU Architectures

LSTM is a type of recurrent neural network that overcomes the issue of gradient vanishing commonly encountered in traditional recurrent networks. By integrating specialized memory cells and gating

mechanisms, LSTM effectively captures and retains long-term dependencies in sequential data. In Figure 2, the inputs and outputs of an LSTM for a single time step are depicted.

Figure 2: Structure of LSTM

The relationships between different components of an LSTM can be described through equations 1-5 [31].

$$f_t = \sigma_g(W_f x_t + U_f h_{t-1} + b_f) \quad (1)$$

$$i_t = \sigma_g(W_i x_t + U_i h_{t-1} + b_i) \quad (2)$$

$$o_t = \sigma_g(W_o x_t + U_o h_{t-1} + b_o) \quad (3)$$

$$c_t = f_t \circ c_{t-1} + i_t \circ \sigma_c(W_c x_t + U_c h_{t-1} + b_c) \quad (4)$$

$$y = o_t \circ \sigma_h(c_t) \quad (5)$$

The parameters associated with the aforementioned relationships are as follows:

W, U	Weight matrices
b	Bias vector
f_t	Forget gate's activation vector
σ_g	Sigmoid function
σ_c, σ_h	Hyperbolic tangent function
x_t	Input vector to the LSTM unit
h_t	Hidden state vector
i_t	Input/update gate's activation vector
o_t	Output gate' activation vector
c_t	Cell state vector
y	Block output

The GRU is a type of recurrent neural network that is similar to LSTM but does not have an output gate. The structure of a GRU is illustrated in Figure 3.

Figure 3: Structure of GRU

Equations 6-9 are related to GRU [32].

$$z_t = \sigma_g(W_z x_t + U_z h_{t-1} + b_z) \quad (6)$$

$$r_t = \sigma_g(W_r x_t + U_r h_{t-1} + b_r) \quad (7)$$

$$\tilde{h}_t = \phi_t(W_h x_t + U_h(r_t \odot h_{t-1}) + b_h) \quad (8)$$

$$h_t = (1 - z_t) \odot h_{t-1} + z_t \odot \hat{h}_t \quad (9)$$

The expressions mentioned above include the following vectors:

x_t	The input vector to the GRU unit
h_t	The output vector to the GRU unit
z_t	The update gate vector
r_t	The reset gate vector
$\hat{h}_t$	The candidate activation vector

The $\odot$ operator denotes the element-wise multiplication.

2.3. Regression Criterion

For assessing the regression performance and continuous estimation of joints, the metrics used were the Pearson correlation coefficient (PCC), root mean squared error (RMSE), and box plots. The PCC quantifies the linear relationship between the predicted and actual values. The RMSE measures the average difference between the forecasted and actual values. Box plots were used to visualize the distribution of predicted and actual values. The PCC and RMSE criteria can be expressed with equations (10) and (11).

$$PCC = \frac{\sum_{i=1}^{n} UV}{\sqrt{\sum_{i=1}^{n} U^2}\sqrt{\sum_{i=1}^{n} V^2}}$$
$$U = y_{pred} - \bar{y}_{pred} \qquad (10)$$
$$V = y_{true} - \bar{y}_{true}$$

$$RMSE = \sqrt{\frac{1}{N}\sum_{i=1}^{n}(y_{pred} - y_{true})^2} \qquad (11)$$

The estimated and actual angles are denoted by y_{pred} and y_{true}. The mean of y_{true} is $\bar{y}_{true}$.

2.4. Preprocessing

This research focused on using LSTM and GRU architectures to estimate finger joint angles based on sEMG data. The preprocessing of sEMG signals has involved the use of synchronization, relabeling, and filtering. High-resolution timestamps were utilized to synchronize the data streams. To be more precise, each stream used either linear or nearest-neighbor interpolation up to the highest sampling frequency. Due to variations in human reaction times and experimental settings, the movements executed by the participants might not align precisely with the stimulus suggested by the software. A generalized likelihood ratio algorithm has been used offline to correct the incorrect movement labels that resulted. Filtering included utilizing a Hampel filter to remove 50 Hz power-line interference from the sEMG signals because the electrodes are susceptible to power-line interferences, which in some cases could alter the recorded signal [28]. The root mean square (RMS) feature was chosen for this study. The expression for the RMS value is given by equation (12):

$$RMS = \sqrt{\frac{\sum_{i=1}^{N} (EMG(i))^2}{N}} \qquad (12)$$

N is the number of measurements.

2.5. Proposed Network Architecture

The suggested networks were constructed using Python. The implementation process involved utilizing two primary tools: TensorFlow, a well-known open-source machine learning framework, and PyCharm, a commonly used integrated development environment for Python programming. TensorFlow was used for constructing and training the networks, whereas PyCharm was utilized as the development environment for coding and testing the implementations. The block diagrams of this design can be observed in Figure 4.

Figure 4: Proposed networks architecture. Three layers of LSTM or GRU, each with 128 cells, make up the network that receives the feature extracted from sEMG signals in the form of an image. There is a dense layer in the final layer.

The input sEMG image has dimensions of $H \times W$ (height × width). Segments of sEMG signals were created using time windows, where the width corresponds to the number of electrodes and the height equals the window length. The window length has been established to 150 milliseconds. The step size, or hop length, between the windows has been chosen to be 10 milliseconds. The target vector in our network consisted of a sequence of finger joint angles that had been collected simultaneously with the sEMG signals. The following are the implemented network parameters: The ADAM optimization algorithm [33] has been used to minimize the loss function. A learning rate of 0.0005 has been selected for the optimization process, which involves 30 iterations. To reduce overfitting, regularization techniques such as dropout with a probability of 0.4 have been implemented. Furthermore, *L2* regularization with a value of 0.0005 has been included to address overfitting issues. Considering the repetitions of the available trials, the data has been split into two parts: training and testing. Each movement has been repeated six times. Two-thirds of the data have been allocated for training, and one-third for testing. This division aims to efficiently assess the model's performance and ensure its generalization capabilities. The signal has been segmented into windows of 150 ms duration.

3. Results

Table 1 displays the total number of parameters and the parameters associated with each layer for both the LSTM and GRU deep neural networks. Notably, the LSTM network has a higher number of parameters compared to the GRU network. The larger parameter count in the LSTM network can be credited to its more intricate architecture, which incorporates additional components like input gates, forget gates, and output gates. These gates introduce extra parameters, resulting in a higher overall parameter count. Although the number of parameters alone does not determine the performance of a neural network, it is interesting to observe the discrepancy in parameter count between the LSTM and GRU networks. This differentiation could

impact the computational complexity and memory requirements in both the training and inference stages of these models. The highest average accuracy in the correlation coefficient measure is 97% for the LSTM network and 85% for the GRU network. The LSTM network requires 30 epochs for training, while the GRU network needs 21 epochs.

Table 1: The total number of parameters, the parameters of each layer, and the characteristics of the two designed networks

Figure 5 (A-D) illustrates the accuracy of joint angle estimation assessed using PCC and RMSE. In the LSTM architecture, the highest accuracy rate for joint angle estimation is achieved at the index MCP joint, reaching an impressive 97% accuracy. The estimation accuracy for angles varies from 83% to 97% based on this criterion. Among the assessed joints, the MCP joint of the thumb shows the least accuracy. Impressively, the index MCP joint attains the highest accuracy, with an RMSE value of 5. RMSE values for all joints fall within the range of 5 to 8. Notably, the thumb MCP joints exhibit the highest error rates based on this specific criterion. Based on the two criteria mentioned earlier, the accuracy of all joints in the LSTM network surpasses that of the GRU network. Figure 6 presents the box diagram depicting the value of the estimated and real joint angles.

Figure 5: Mean PCC and RMSE associated with the estimation of joint angles during the M1-M6 movements

Figure 6: Compare estimated and real of fingers interphalangeal joints angles: (A) Thumb MCP joint, (B) Thumb PIP joint, (C) Index MCP joint,(D) Index PIP joint, (E) Index DIP joint, (F) Middle MCP joint, (G) Middle PIP joint, (H) Ring MCP joint, (I)Ring PIP joint, (J) Ring DIP joint, (K) Pinky MCP joint, (L) Pinky PIP joint, (M) Pinky DIP joint.

Figure 7 displays the prediction and test angles of finger joints during M1-M6 movements performed by an individual.

Figure 7: The interphalangeal joint angles for subject 1(A) Index PIP joint angle-fist, (B) Middle PIP joint angle-fist, (C) Middle PIP joint angle-pointing, (D) Ring PIP joint angle-pointing, (E) Little DIP joint angle-pointing, (F) Index MCP joint angle-thumb up, (G) Ring PIP joint—thumb up, (H) Pitch wrist joint angle—V movement. The outcomes are associated with the recommended LSTM network.

4. Discussion

This research introduces a deep learning model for estimating finger angles using sEMG signals. Since movement information changes over time, it is crucial for the model to capture temporal dependencies. LSTM and GRU networks are particularly suited for analyzing time series data due to their ability to handle these

temporal dependencies. LSTM networks are equipped with a separate output cell state, which allows them to store and output different information. On the other hand, GRU networks have a single hidden state that serves both as a memory and for output. The findings of the study indicate that the LSTM model accurately predicts finger angles during continuous M1-M6 movements.

Hand and finger movements are primarily controlled by the muscles situated in the forearm. Figure 8 illustrates the relationship between muscles and the corresponding finger joints in the human forearm. Finger bending is carried out by the flexor muscles. Within the lower forearm region, the *flexor digitorum superficialis* and *flexor digitorum profundus* muscles play a significant role in flexing the index, middle, ring, and little fingers. Moreover, in the group of *thenar* muscles, two sets of flexor muscles play a role in bending the thumb. The flexion of the thumb is governed by the *flexor pollicis longus* muscle. It is situated deep within the hand. The extensor muscles are responsible for straightening the fingers. These are on the back of the forearm. The *extensor digitorum* muscle, responsible for extending the fingers except for the thumb, is a superficial muscle.

Figure 8: Flexor and Extensor muscles of the forearm [34]

Alongside this muscle, the *extensor digiti minimi* muscle contributes to the extension of the little finger, also being superficial. The extensor indicis muscle, a deep muscle, is essential for extending the index finger. Thumb extension involves two deep muscles, the *extensor pollicis brevis* and *extensor pollicis longus* [34]. M1-M6 movements have been created by combining finger flexion and extension movements. Based on the electrode placement, the sEMG signals obtained from electrodes placed on the forearm provide sufficient information about the movements of the non-thumb fingers. This allows for precise estimation of the angles of the finger joints (excluding the thumb) with a high level of precision. However, it should be noted that the electrodes are not positioned directly on the muscles responsible for thumb flexion. Therefore, the corresponding sEMG signal lacks sufficient richness of information, making it challenging to accurately estimate the angles of the intermediate joints of the thumb. Additionally, the index and little fingers have an additional extensor muscle. This observation is further supported by the results presented in the results section of the article. Comparing similar works can be a complex task, but it is essential for understanding the advancements in a particular field. He et al. used a muscle synergy-based musculoskeletal model and 32 electrodes. They achieved the highest accuracy of 0.92 precisely [4]. Stapomchaisit et al. developed a method to predict finger joint angles based on the correlation coefficient criterion, achieving an accuracy exceeding 0.7. Their approach involved utilizing 128 electrodes and applying the independent components of the sEMG signal to a linear regression model [9]. Zhang et al. achieved an accuracy of 0.91 in predicting MCP joint angles. In their research, they utilized six electrodes and applied Gaussian process regression to establish the correlation between sEMG features and hand kinematics [11]. Chen et al. forecasted finger kinematics by analyzing motor unit discharge times using high-density electrodes, achieving an accuracy of 85% [12]. Pallotti et al. estimated the maximum accuracy of 0.87 for the MCP joint in four grasp movements [14]. In a study by Dai et al., the extension angles of the MCP joints were approximated using 160 electrodes. Their methodology involved a two-step process: initially classifying finger movements and subsequently utilizing second-order polynomial regression to predict the angles of the joints. Their study showed that the estimation accuracy of these joint angles is above 0.8 [15]. Roy et al. decomposed sEMG signals of the extrinsic finger muscles. By utilizing 128 electrodes in their experimental setup, they achieved an accuracy of 0.94 in

predicting the joint angles [16]. Guo et al. achieved a maximum accuracy of 0.82 in their research, as determined by the correlation coefficient metric [24]. Wang et al. focused on six grasp movements and reported a maximum accuracy of 0.9 [25]. Avian et al. reported an overall accuracy of 0.95 in the MCP joint but did not provide specific results regarding the accuracy of each joint and their respective kinematics [27]. Some of the previously mentioned research dealt with the decomposition of EMG signals into motor units [4, 9, 12, 15, 16], which was valuable work, but it required a large number of electrodes and was complicated and time-consuming. Several earlier studies also employed traditional machine learning methods [11, 14], which were costly and time-consuming and could result in the loss of important signal information [17, 35]. Several of the above studies only looked at the kinematics of a single joint or a small number of joints [11, 15, and 27].

All of the interphalangeal joint angles of every finger have been estimated in the current study using just ten electrodes. LSTM deep neural networks and one of their well-known variations have been researched to take into account the nature of EMG signals. With 97% accuracy, the majority of the joints are anticipated. Physiological analysis has been used to determine why thumb joints are assessed less accurately than those of other fingers. All of the constructed network's hyperparameter, as well as the ideal window length for the windowing approach in network performance analysis, are specified in this study.

In terms of the number of gates, LSTM has three gates: the Forget Gate, the Input Gate, and the Output Gate. These gates independently control values, allowing long-term and short-term memory to be managed effectively. GRU, on the other hand, has two gates: the Update Gate and the Reset Gate. GRU's structure is simpler and does not require separate gates for input and forget operations. From a complexity perspective, LSTM is more complex compared to GRU. Due to having more parameters, it performs heavier computations. In contrast, GRU has a simpler architecture with fewer parameters, making it faster to train and requiring fewer computations. In terms of memory capacity, LSTM maintains two separate memories: the Cell State and the Hidden State. This enables it to store information for longer durations. In comparison, GRU uses only one shared memory, the Hidden State, resulting in more compact information storage. Regarding speed and performance, GRU, due to its simpler structure and fewer parameters, trains faster and requires less memory. However, LSTM typically achieves higher accuracy but takes more time to train.

According to the glove's datasheet, these sensors' resolution is less than 1 degree. Considering the number of electrodes and their placement, the amount of information obtained from them can, at best, lead to predictions with this level of accuracy.

5. Conclusion

In this investigation, promising outcomes have been attained in estimating the angles of the joints of the fingers. A comprehensive physiological analysis was presented to elucidate the variations in the accuracy of interphalangeal joint angle estimation and to investigate the muscles that impact joint movement. Given the sequential nature of sEMG signals, deep recurrent neural networks are the preferred choice. Among these networks, the LSTM network surpasses the GRU. This aspect was explored in the current study.

In addition to the isometric and isotonic movements examined in this study, flexion and extension movements are also considered fundamental motions. In future research, this topic will be further explored, and the estimation of joint angles in these types of movements will also be investigated. One of the key factors in enhancing the performance of deep neural networks based on LSTM cells is the application of regularization techniques. Moreover, selecting the optimal window length in the windowing method significantly impacts the performance of these networks and will be thoroughly studied in future research. Additionally, LSTM

and GRU cells feature bidirectional architecture. Investigating and evaluating these cells to better understand their performance in achieving higher estimation accuracy can be a valuable area for future studies.

References

1. A.Ayyad, A. M., A.Owida, H., D. Fazio, R., et al. "Electromyography Monitoring systems in Rehabilitation: A review of clinical applications, wearable devices and signal acquisition methodologies", *Electronics*, 12, 7 (2023). https://doi.org/10.3390/electronics12071520.
2. M.Sarhan, S., Z.Al-Faiz, M., Takhakh, M. "A review on EMG/EEG based control scheme of upper limb rehabilitation robots for stroke patients", *Heliyon*, 9, 8 (2023). https://doi.org/10.1016/ j.heliyon. 2023.e18308.
3. Kamavuako, EN. "On the Applications of EMG Sensors and Signals", *Sensors (Basel)*. 2022 Oct 19; 22 (20):7966. https://doi.org/10.3390/s222 07966.
4. He, Z., Qin, Z., Koike, Y. "Continuous Estimation of Finger and Wrist Joint Angles Using a Muscle Synergy Based Musculoskeletal Model", *Appl. Sci*, 12, 3772 (2022). https://doi.org/10.3390/app1208 3772
5. Kim, Y., Staporchaisit, S., Kambara, H., et al. "Muscle synergy and musculoskeletal model-based continuous multi-dimensional estimation of wrist and hand motions", *Journal Healthcare Engineering*, 5451219 (2020). https://doi.org/10.1155/2020 /5451 219.
6. Ma, X., Liu, Y. "Continuous estimation of knee joint angle based on surface electromyography using a Long Short-Term Memory neural network and time- advanced feature", *Sensors*, 20, 17 (2020). https://doi.org/10.3390/s 20174966.
7. Gao, Y., Luo, Y., Zhao, J., et al. "sEMG-angle estimation using feature engineering techniques for Least Square Support Vector Machine", *J. Technol. Health Care*, 27, s1, pp. 31-46, (2019). https://doi.org/10. 3233/thc-199005.
8. Savithri, C. N., Priya, E., Rajasekar, K. "A machine learning approach to identify hand actions from single-channel sEMG signals", *Biomedical engineering- Biomedizinische Technik*. 2022; 67 (2), 89–103. https://doi.org/10.1515/bmt-2021-0072
9. Staporchaisit, S., Koike, Y., Takagi, A., et al. "Finger angle estimation from array EMG system using linear regression model with independent component analysis", *Front. Neurorobot*, 13, 75 (2019). https://doi.org/ 10.3389/fn bot.2019.00075.
10. Veer, K., Vig R. "Identification and classification of upper limb motions using PCA", *Biomedical Engineering/ Biomedizinische Technik*. 2018; 63(2): 191-196. https://doi.org/10.1515/bmt-2016-0224.
11. Zhang, Q., Pi, T., Liu, R., et al. "Simultaneous and proportional estimation of multijoint kinematics from EMG signals for myo control of robotic hands", *IEEE/ASME Trans. Mechatronics*, 25, 4, pp. 1953-60, (2020). https://doi.org/10.1109 /mech. 2020.2999532.
12. D., Zhu, X. "Prediction of finger kinematics from discharge timings of motor units: Implications for intuitive control of myoelectric prostheses", *J. of Neural Eng*, 16, 2 (2019). https://doi.org/10.1088 / 17 41-2552/aaf4c3.
13. Hu, X., Song, A., Wang, J., et al. "Finger movement recognition via High-Density electromyography of intrinsic and extrinsic hand muscles", *Scientific Data*, 9,373 (2022). https:// doi.org/10.1038/ s41597-022-01484-2.
14. Pallotti, A., Orengo, G., Saggio, G. "Measurements comparison of finger joint angles in hand postures between a sEMG armband and a sensory glove", *Biocybernetics and Biomedical Engineering*, 41, 2, pp. 605–616, (2021). https://doi.org/10.1016 /j.bbe. 2021.03.003 .
15. Dai, C., Hu, X. "Finger joint angle estimation based on motor neuron discharge activities", *IEEE J. Biomed. Heal. Informatics*, 24, 3, pp. 760–67, (2020). https://doi.org /10.1109/jbhi.2019.2926307.
16. Roy, R., Zheng, Y., D. G. Kamper, D. G., et al. "Concurrent and Continuous Prediction of Finger Kinetics and Kinematics via Motoneuron Activities", *IEEE Transactions on Biomedical Engineering*, 70(6): pp. 1911-1920, (2023) .https://doi.org/10.1109/TBME. 2022. 323 2067.
17. Tufail, S. "Advancements and Challenges in Machine Learning: A Comprehensive Review of Models, Libraries, Applications, and Algorithms", *Electronic*, (2023). https:// doi.org/10.3390/elect ronics12081789.
18. Batayneh, W., Abdulhay, E., Alothman, M. "Prediction of the performance of artificial neural networks in mapping sEMG to finger joint angles via signal pre-investigation techniques", *Heliyon*, 6, 4 (2020). https://doi.org/10.1016/j.heliyon.2020.e03669.
19. Gao, Z., Tang, R., Huang, Q., et al. "A multi-DoF prosthetic hand finger joint controller for wearable sEMG sensors by nonlinear autoregressive exogenous model", *Sensors*, 21(8), 2576 (2021). https://doi.org/10.3390/s21 082576.
20. Hu, Y., Wong, Y., Wei, W, et al. "A novel attention based hybrid CNN-RNN architecture for sEMG-based gesture recognition", *PLOS ONE*, 13, 10 (2018). https://doi.org/10.1371/journal . pone. 0206049.
21. Rezaei Nezhad H., Keynia, F., Sabbagh Molahosseini, A., "Optimized deep networks structure to improve the accuracy of estimator algorithm in deep networks learning", *Scientia Iranica*, 31(5), pp. 417-429 (2024). https://doi.org / 10.24200/sci.2023.62337. 7782.
22. Moradi, M.M., Fatehi, M.H., Masoumi, H., et al. "Deep neural network method for classification of sleep stages using spectrogram of signal based on transfer learning with different domain data", *Scientia Iranica*, 29(4), pp. 1898-1903 (2022). https://doi.org/10.24200/sci.2022. 58204.5613.

23. Wen, Y., Kim, S.J., Avrillon, S., et al. “A deep CNN framework for neural drive estimation from HD-EMG across contraction intensities and joint angles”, *IEEE Transactions Neural System Rehabilitation Engineering*; 30, pp. 2950-59, (2022). https://doi.org/10.1109/tnsre.2022.321524 6.
24. Guo, W., Ma, C., Wang, Z., et al. “Long exposure convolutional memory network for accurate estimation of finger kinematics from surface electromyographic signals”, *J Neural Eng*, 3(18) (2021). https://doi.org /10.10 88/1741-2552/abd46 1.
25. Wang, C., Guo, W., Zhang, H., et al. “sEMG based continuous estimation of grasp movements by long-short term memory network”, *Biomedical and Signal Processing Control* 59 (2020). https://doi. org/10.1016/j.bspc.2019.101774
26. Chen, Y., Yu, S., Ma, K., et al. “A continuous estimation model of upper limb joint angles by using surface electromyography and deep learning method”, *IEEE Access*. 7, pp.174940-50, (2019). https://doi.org/10.1109/ access.2019.2956951.
27. Avian, C., Prakosa, S.W., Faisal, M., et al. “Estimating finger joint angles on surface EMG using manifold learning and Long Short-Term Memory with attention mechanism”, *Biomedical Signal Processing and Control*. 71 (2022). https://doi.org/ 10.1016/ j.bspc.2021 . 103099.
28. Atzori, M., Gijsberts, A., Castellini, C. et al. “Electromyography data for non-invasive naturally-controlled robotic hand prostheses”, *Sci Data*. 1, 140053 (2014). https://doi.org/10.1038/sdata.20 14.53.
29. Atzori, M., A. Gijsberts. “Characterization of a benchmark database for myoelectric movement classification”, *IEEE Transactions Neural Systems Rehabilitation*. 23(1): 73-83, (2013). https://doi. org/10.110 9/tnsre.2014.2328495.
30. Jarque-Bou N.J, Atzori M, Müller H. “A large calibrated database of hand movements and grasps kinematics”, *Sci. Data*. 7(12), (2022). https://doi. org/10.1038 /s41597-019-0349-2 .
31. Greff, K., Srivastava, R.K. “LSTM: A Search Space Odyssey”, *IEEE Transactions Neural Networks and Learning Systems*. 28(10) pp. 2222-32, (2016). https://doi.org/10.1109/tnnls.2016. 2582924.
32. Chung, J., Gulcehre, C., Cho, K., et al. “Empirical evaluation of gated recurrent neural networks on sequence modeling”. *ArXiv: 1412.3555* (2014). https://doi.org/10. 48550/ arXiv.1412.3555.
33. Kingma, D.P., Ba, J.L. Adam: “A method for stochastic optimization”, *In Proc. Int. Conf. Learning Representations, San Diego, USA.* pp. 7-9, (2019). https://doi.org/10.48550/arXiv.1412. 6980.
34. Hirt, B., Seyhan, H., Wagner, M., et al. “Hand and Wrist Anatomy and Biomechanics, a Comprehensive Guide”. 3nd ed., Germany, *Thieme*. pp. 75-80, (2017).
35. Kanjilal, R., Uysal, I. “The future of human activity recognition: Deep Learning or feature engineering”, *Neural Processing Letters*, 53, pp. 561-579, (2021). https:// doi.org/10.1007/s11063-020-10400-x.

Figure 1: (A): The placement of electrodes [28]. (B): Selected movements of the fingers [29]. (C): The placement of bending sensors [30]

Figure 2: Structure of LSTM

Figure 3: Structure of GRU

Figure 4: Proposed networks architecture. Three layers of LSTM or GRU, each with 128 cells, make up the network that receives the feature extracted from sEMG signals in the form of an image. There is a dense layer in the final layer.

Table 1: The total number of parameters, the parameters of each layer, and the characteristics of the two designed networks

(A) The mean PCC using the LSTM network

(B) The mean PCC using the GRU network

(C) The mean RMSE using the LSTM network

(D) The mean RMSE using the GRU network

Figure 5: Mean PCC and RMSE associated with the estimation of joint angles during the M1-M6 movements

Figure 6: Compare estimated and real of fingers interphalangeal joints angles: (A) Thumb MCP joint, (B) Thumb PIP joint, (C) Index MCP joint, (D) Index PIP joint, (E) Index DIP joint, (F) Middle MCP joint, (G) Middle PIP joint, (H) Ring MCP joint. (I)Ring PIP joint, (J) Ring DIP joint, (K) Pinky MCP joint, (L) Pinky PIP joint, (M) Pinky DIP joint.

Figure 7: The interphalangeal joint angles for subject 1 (A) Index PIP joint angle-fist, (B) Middle PIP joint angle-fist, (C) Middle PIP joint angle-pointing, (D) Ring PIP joint angle-pointing, (E) Little DIP joint angle-pointing, (F) Index MCP joint angle-thumb up, (G) Ring PIP joint—thumb up, (H) Pitch wrist joint angle—V movement. The outcomes are associated with the recommended LSTM network.

Figure 8: Flexor and Extensor muscles of the forearm [34]

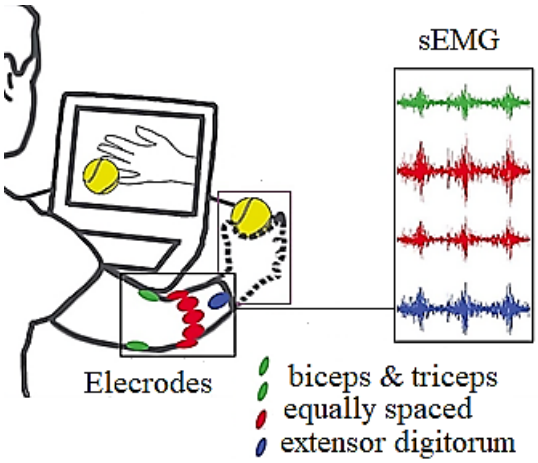

A

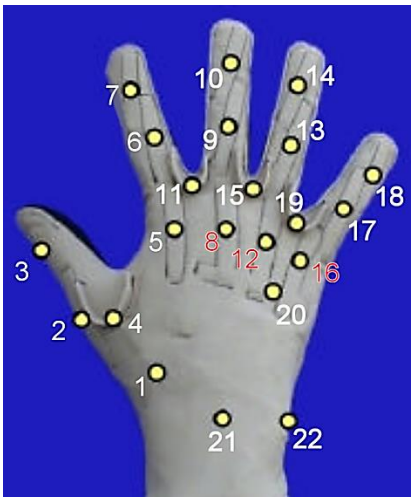

C

M1- Thumb up

M2-V

M3- Pointing

M4-Finger flexed & fist

M5- Flexion of ring & pinky

M6-Thumb opposing pinky

B

Figure 1

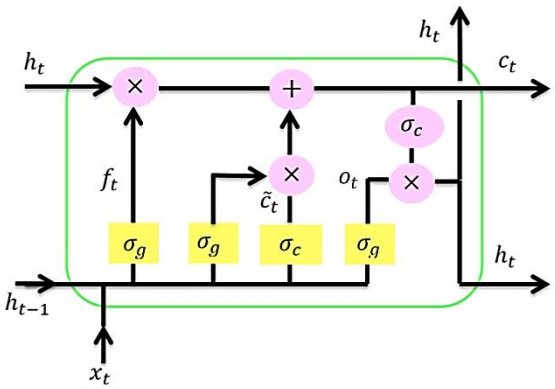

Figure 2

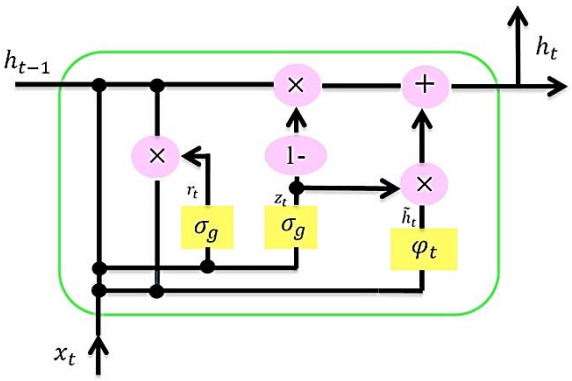

Figure 3

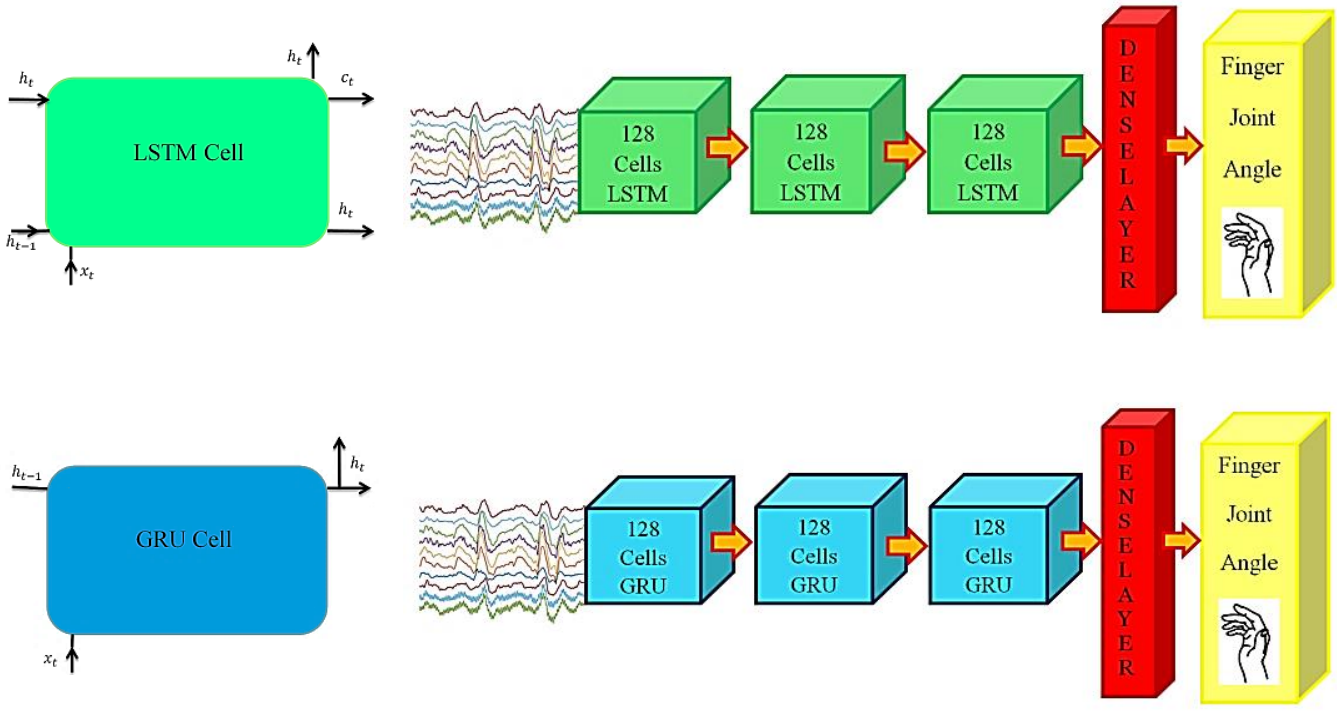

Figure 4

Table 1

Type cells	LSTM	GRU
Total parameters	254000	194634
Hidden layer	71168	53376
Hidden Layer	131584	98688
Dense Layer	51248	42570
Iteration	30 Epoch	21 Epoch
Accuracy(PCC)	97%	85%
Learning time	75 minute	30 minute
Number gates per each cell	3	2

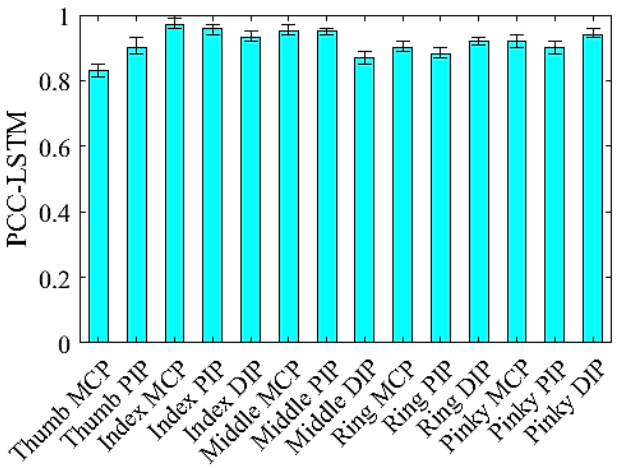

(A) The mean PCC using the LSTM network

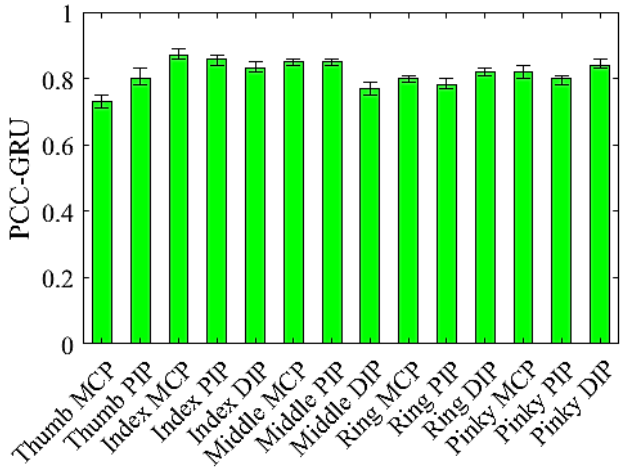

(B) The mean PCC using the GRU network

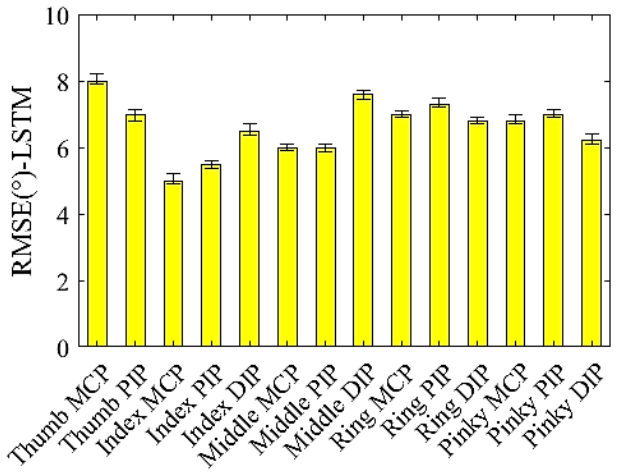

(C) The mean RMSE using the LSTM network

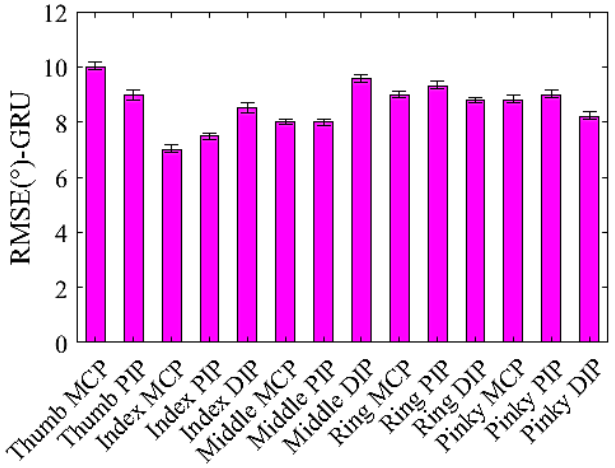

(D) The mean RMSE using the GRU network

Figure 5

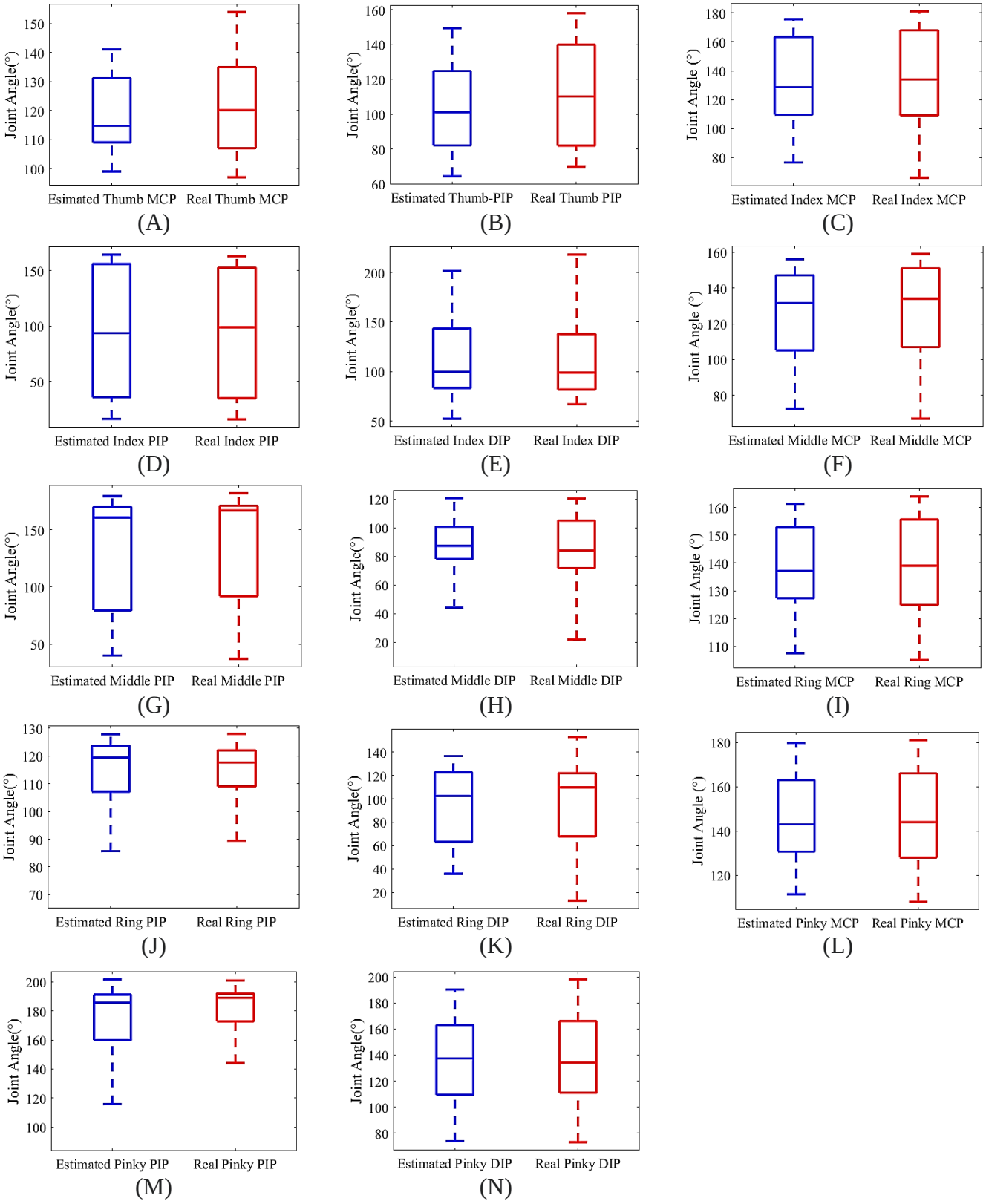
Joint Angle(°)
Esimated Thumb MCP
Real Thumb MCP
(A)
Joint Angle(°)
Estimated Thumb-PIP
Real Thumb PIP
(B)
Joint Angle (°)
Estimated Index MCP
Real Index MCP
(C)
Joint Angle(°)
Estimated Index PIP
Real Index PIP
(D)
Joint Angle(°)
Estimated Index DIP
Real Index DIP
(E)
Joint Angle (°)
Estimated Middle MCP
Real Middle MCP
(F)
Joint Angle(°)
Estimated Middle PIP
Real Middle PIP
(G)
Joint Angle(°)
Estimated Middle DIP
Real Middle DIP
(H)
Joint Angle (°)
Estimated Ring MCP
Real Ring MCP
(I)
Joint Angle(°)
Estimated Ring PIP
Real Ring PIP
(J)
Joint Angle(°)
Estimated Ring DIP
Real Ring DIP
(K)
Joint Angle (°)
Estimated Pinky MCP
Real Pinky MCP
(L)
Joint Angle(°)
Estimated Pinky PIP
Real Pinky PIP
(M)
Joint Angle(°)
Estimated Pinky DIP
Real Pinky DIP
(N)

Figure 6

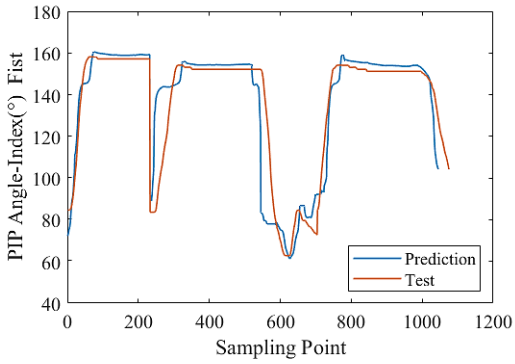

(A)

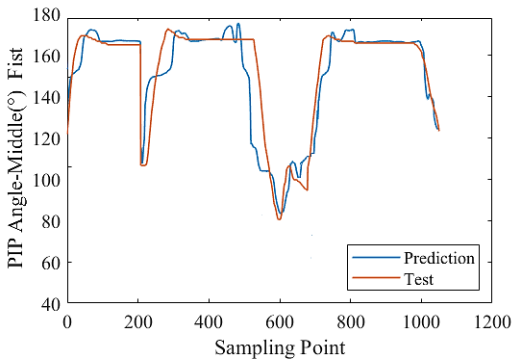

(B)

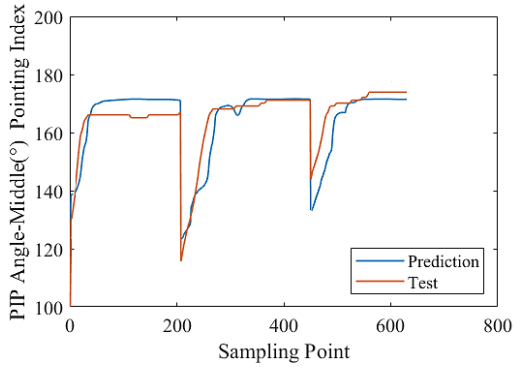

(C)

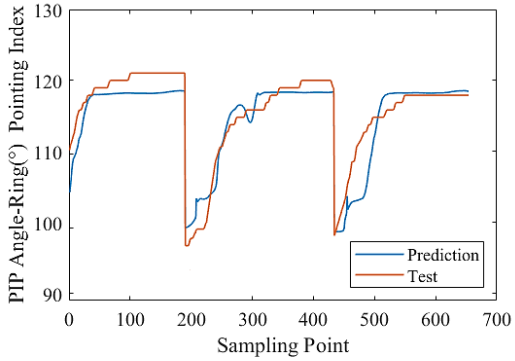

(D)

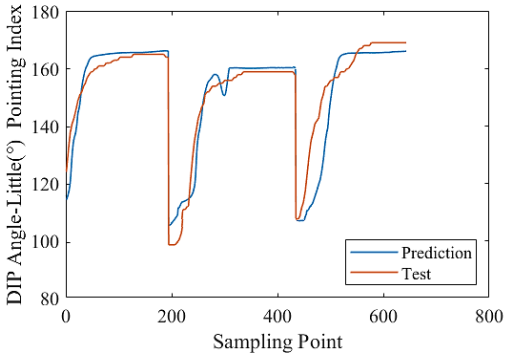

(E)

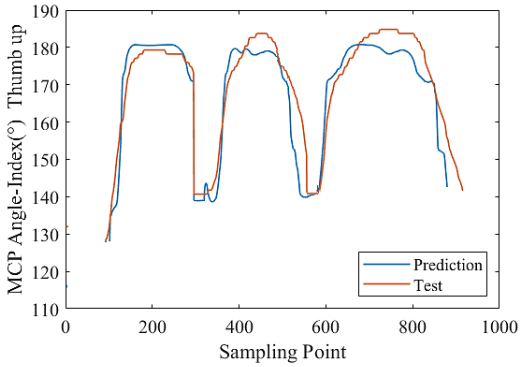

(F)

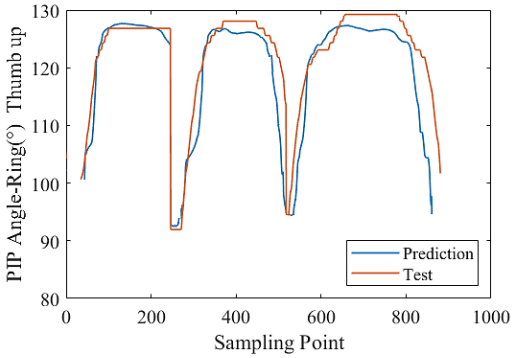

(G)

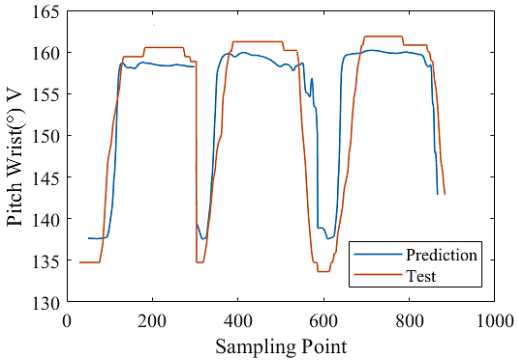

(H)

Figure 7

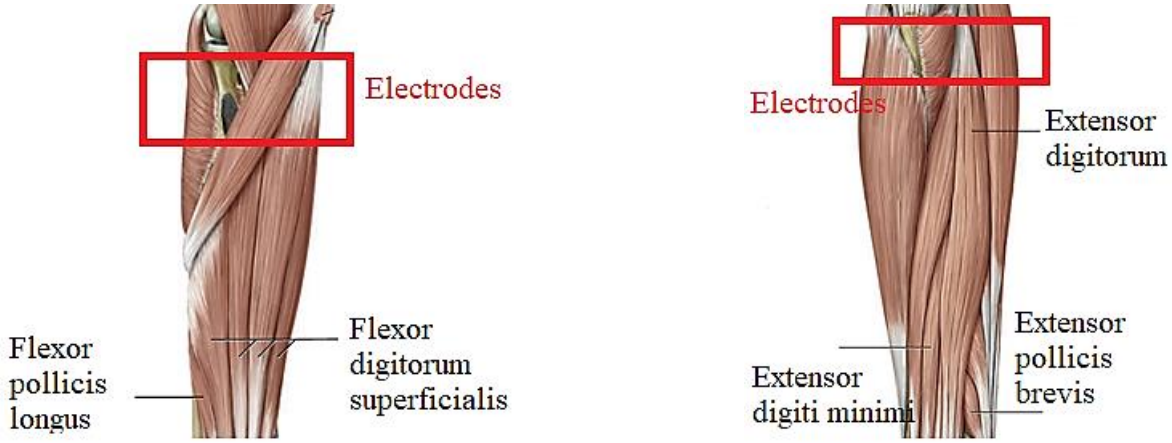
Electrodes
Flexor pollicis longus
Flexor digitorum superficialis
Electrodes
Extensor digitorum
Extensor pollicis brevis
Extensor digiti minimi

Figure 8

Masoud Saheb Jameyan, Ph.D. Candidate

Biomedical Eng. Department,
Amirkabir University of Tech,
424 Hafez Ave.,
Tehran, Iran.
Postal Box: 15875-4413
Cell: (+98) 912-8063375
Email: sjameyan@aut.ac.ir

Mohammad Ali Ahmadi-Pajouh, Ph.D.

Biomedical Eng. Department,
Amirkabir University of Tech,
424 Hafez Ave.,
Tehran, Iran.
Postal Box: 15875-4413
Cell: (+98) 912-6304792
Work: (+98)21-64545570,
Email: pajouh@aut.ac.ir

Mohammad Hassan Moradi, Ph.D.

Biomedical Eng. Department,
Amirkabir University of Tech,
424 Hafez Ave.,
Tehran, Iran.
Postal Box: 15875-4413
Work: (+98)21-64542399,
Email: mhmoradi@aut.ac.ir

Biography

Masoud Saheb Jameyan

Masoud Saheb Jameyan obtained his bachelor's and master's degrees in Control Electrical Engineering and Electronics Electrical Engineering from Isfahan University of Technology and Noshirvani University of Technology, respectively. He is currently a Ph.D. candidate in Biomedical Engineering (Bioelectric) at Amirkabir University of Technology. His Ph.D. research focuses on the classification and regression of human hand and finger movements using electromyogram signals, machine learning, and deep learning. He has expertise in designing digital electronic boards, machine learning, and deep learning.

Mohammad Ali Ahmadi-Pajouh

Dr. Mohammad Ali Ahmadi-Pajouh is an accomplished researcher and academic specializing in biomedical engineering, with a focus on human motion analysis and cognitive modeling. He earned his Ph.D. in Biomedical Engineering from Amirkabir University of Technology, Tehran, Iran, in 2012. His doctoral research centered on estimating human arm stiffness using kinematic

and electromyogram signals, highlighting his expertise in integrating biomechanics and signal processing. During his Ph.D., Dr. Ahmadi-Pajouh was also a visiting scholar at Johns Hopkins University, USA, where he explored the context-dependent modulation of sensory feedback gains. His earlier academic achievements include a Master's degree in Biomedical Engineering from Amirkabir University and a Bachelor's degree in Electrical Engineering (Control Engineering) from K.N. Toosi University of Technology.

Since 2013, Dr. Ahmadi-Pajouh has served as an Assistant Professor in the Biomedical Engineering Department at Amirkabir University of Technology. Additionally, he has contributed to interdisciplinary research as a faculty member of the Independent Mechatronics Group and previously at the Iranian Research Institute for Cognitive Sciences. His work spans cognitive modeling, human path planning, and sensory-motor control, combining his engineering background with innovative approaches to understanding human movement and behavior. Dr. Ahmadi-Pajouh's ongoing research reflects his commitment to advancing biomedical engineering and cognitive science.

Mohammad Hassan Moradi

Mohammad Hassan Moradi received his B.Sc. and M.Sc. degrees in Electronic Engineering from University of Tehran, Iran, in 1988 and 1990, respectively. He received his PhD degree from Tarbiat Modarres University, Tehran, Iran, in 1995. He has been with the faculty of biomedical engineering, Amirkabir University of Technology, Tehran, Iran, since 1995. His primary research and teaching interests include design, manufacturing and application of medical instrumentation, biomedical signal processing, cognitive
neuroscience, neuro-marketing, wavelet system design, time-frequency transforms and deep fuzzy neural systems. He has published over 200 technical papers in various high impact factor peer-reviewed journals. Moreover, he presented more than 400 papers in international conferences. Professor Moradi translated a book on wavelet signal processing into Persian. He has written 20 book chapters as well.